Application of Fermi hypernetted-chain theory to spin-polarized higher-order fractional quantum Hall states

J. W. Kim
Da Vinci College of General Education, Chung Ang University, Seoul 06974, Korea

H. Kim and N. Kim[*]
Department of Physics, Soongsil University, Seoul 06978, Korea

(Received 17 November 2016; revised manuscript received 14 February 2017; published 6 April 2017)

We apply Fermi hypernetted-chain theory to study the spin polarization of higher-order fractional quantum Hall (FQH) states at filling factors in between the primary FQH sequences, $\nu = p/(q_e p \pm 1)$, where q_e is an even integer and p is a nonzero integer. The filling factors related to the higher-order FQH states include $\nu = 3/8$, $4/11$, $5/13$, $5/17$, $4/13$, $6/17$, $7/11$, and so on. We use a model of strongly interacting fermions with different spin degrees of freedom to explain the states beyond primary FQH sequences. We calculate the correlation energy, the radial distribution function, as well as the static structure function associated with the Halperin wave function adopted for the mixture states of fermions with different spins. The results are comparable with those from the residual interaction between composite fermions.

DOI: 10.1103/PhysRevB.95.155109

I. INTRODUCTION

The fractional quantum Hall effect [1] (FQHE) results from a strongly correlated incompressible fluid state [2] formed in a two-dimensional electron-gas (2DEG) system with special uniform electron densities ρ in the extreme limit of a strong transverse magnetic field ($B > 5$ T), low temperature ($T < 2$ K), and high mobility of electrons ($\mu > 10^5\ \mathrm{cm}^2\ \mathrm{V/s}$). From a theoretical point of view, it was originally assumed that the Zeeman splitting is sufficiently large such that the spins of all electrons in the Landau level at filling factors of the form $\nu = 1/m$ ($m = 1,3,5,\cdots$) are completely polarized [3]. However, due to the small effective electron mass m_b^* ($m_b^* = 0.067 m_e$, m_e the electron mass) and the small g factor ($g = -0.44$), in GaAs the Zeeman term is about 70 times smaller than the cyclotron energy $\hbar\omega_c$ (for GaAs, $\hbar\omega_c = 20B$ in Kelvin, with B in Tesla) [4]. Meanwhile, FQHE can also be observed at relatively low magnetic fields, where the Coulomb energy scale can easily mix the different spin channels. The interaction energy, which is roughly of the same order as the cyclotron energy for typical experimental parameters, is also much larger than the Zeeman energy. Therefore, it may sometimes be energetically favorable for finite particles to reverse their spins, provided that they can gain more in interaction energy than they lose in Zeeman energy. Exact diagonalization studies on small systems [5–12] confirmed that this does indeed occur at sufficiently low Zeeman energy. There have also been experimental investigations [13–31] of the nonfully spin polarized FQH states as well as transitions between them as a function of the Zeeman energy.

For the primary FQH sequences, $\nu = p/(q_e p \pm 1)$, where p is a nonzero integer and q_e is an even integer, the composite fermion (CF) model [32–35], proposed by Jain, has been very successful around major even-denominator fractions, $\nu = 1/q_e$ ($p \to \infty$). In this model, the dominant Coulomb interaction between carriers in a 2DEG system in high magnetic fields is very effectively incorporated by the adiabatic capture of an even number q_e of magnetic flux quanta to each electron. This gives rise to composite fermions as quasiparticles. The CF model is a remarkably simple picture in which CFs can be regarded as independent particles in an effective magnetic field, $B^* = B - q_e\phi_0\rho$, which is reduced from the external magnetic field B by the density ρ of the captured magnetic flux, where $\phi_0 = hc/e$ is the magnetic flux quantum. At special filling factors $\nu = \phi_0\rho/B = 1/q_e$ the effective magnetic field B^* vanishes, so the system of CFs can be described as free fermions in a zero magnetic field, characterized by a Fermi wave vector and a Fermi energy. When B^* deviates from zero, Landau levels p of CFs develop, giving rise to an integer quantum Hall effect (IQHE) of noninteracting composite fermions. This IQHE of CFs in the effective magnetic field becomes equivalent to the FQHE of the original interacting electrons exposed to the external magnetic field.

However, as experimental conditions are improved, higher-order FQH states are observed at filling factors $\nu = 4/11$, $5/13$, $6/17$, $4/13$, $5/17$, and $7/11$, which lie in between the primary FQH states (IQH states of CFs) [23,24,28] $\nu = 2/3$ and $2/7$ by Pan *et al.* [24,25], and observed at $\nu = 3/8$ in the photoluminescence spectra of 2DEG by Bellani *et al.* [26]. Further, in a recent experiment, higher-order filling factors in the region of $1/3 < \nu < 2/5$, as $\nu = 5/13$, $6/17$, and $3/8$, have been observed by Samkharadze *et al.* [27]. As a consequence, assuming q_e vortices bound to each CFs, the filling factor ν^* of new incompressible CFs states caused from the interaction between CFs is produced from the relation of $\nu = \nu^*/(q_e\nu^* \pm 1)$ [36]. For example, $\nu = 4/11$ and $6/17$ correspond to $\nu^* = 1 + 1/3$ and $1 + 1/5$, respectively, indicating fractional fillings in the topmost CF Landau level. In a model for partially spin-polarized QHE with respect to this problem, the residual interaction between CFs, which occupy only the topmost CF Landau level with fractional filling [36,37], can be responsible for the higher-order FQHE.

In this paper we adopt a model of strongly interacting two types of fermions to study the spin polarization of

[*]nammee@ssu.ac.kr

FQH states at filling factors, which are located in between primary FQH states. For numerical calculation we apply Fermi hypernetted-chain (FHNC) theory to the Halperin wave function (HWF) [2,4] with SU(2) symmetry. In contrast to the CF model, we know that the HWF does not cover all the representation of FQH states at filling factors $\nu = p/(q_e p \pm 1)$. Nonetheless, the HWF may be a good candidate for the investigation of spin-polarized FQH states at higher-order filling factors in the regime $2/3 > \nu > 2/7$.

The HWF for a system of two types of strongly interacting fermions, i.e., consisting of $N^\uparrow$ spin-up (major) electrons and $N^\downarrow$ spin-down electrons ($N = N^\uparrow + N^\downarrow$), is given by

$$\Psi_{lmq}(\mathbf{R}^\uparrow,\mathbf{R}^\downarrow) = \prod_{i<j}^{N^\uparrow}(z_i^\uparrow - z_j^\uparrow)^l \prod_{i<j}^{N^\downarrow}(z_i^\downarrow - z_j^\downarrow)^m \prod_{i,j}^{N^\uparrow,N^\downarrow}(z_i^\uparrow - z_j^\downarrow)^q \times \prod_i^{N^\uparrow} e^{-\frac{|z_i^\uparrow|^2}{4\ell_0^2}} \prod_j^{N^\downarrow} e^{-\frac{|z_j^\downarrow|^2}{4\ell_0^2}}, \tag{1}$$

where $\mathbf{R}^\sigma$ denotes coordinates $(z_1^\sigma, z_2^\sigma, \ldots, z_{N^\sigma}^\sigma)$ of all spin σ electrons, $z_i = x_i + \mathrm{i}y_i$ is the position of the ith electron in complex coordinates, $\ell_0 = (c\hbar/eB)^{1/2}$ is the magnetic length, l and m are odd integers, and q is an integer. By construction, neglecting Landau-level mixing, this wave function lies entirely in the lowest Landau level (LLL) and describes a translational invariant isotropic and incompressible liquid of electrons at the LLL filling factor

$$\nu = \nu^\uparrow + \nu^\downarrow = \frac{l + m - 2q}{lm - q^2}. \tag{2}$$

The filling factors $\nu^\uparrow$ and $\nu^\downarrow$ are, respectively, determined as

$$\nu^\uparrow = \frac{m - q}{lm - q^2}, \quad \nu^\downarrow = \frac{l - q}{lm - q^2}. \tag{3}$$

Therefore, the spin polarization ζ of FQH states at a filling factor ν is defined as

$$\zeta = \frac{\nu^\uparrow - \nu^\downarrow}{\nu^\uparrow + \nu^\downarrow} = \frac{m - l}{m + l - 2q}, \tag{4}$$

where q is an integer with the restriction of $q < l,m$, due to $0 \leqslant \zeta \leqslant 1$. For the case of the fully spin-polarized state ($\zeta = 1$), by eliminating one of the spin components in Eq. (1), this wave function becomes the Laughlin wave function for spinless (as fully spin polarized) electrons, which describes the electronic state at filling factor $\nu = 1/m$. With a choice of $l = m$, the electronic states in the LLL at filling factors $\nu = 2/(l + q)$ are spin unpolarized, ($\zeta = 0$); otherwise, the states are partially spin polarized ($\zeta < 1$). For example, the spin polarization of the FQH state at filling factor $\nu = 4/11$ is determined as the spin polarization $\zeta = 3/4$ by construction of $(l,m,q) = (3,15,1)$ and $\zeta = 1/2$ with $(l,m,q) = (3,5,2)$. The electronic state at filling factor $\nu = 4/11$ with $\zeta = 1/2$ is more energetically favorable than the others (see Sec. III). Furthermore, we can also find a good trial wave function for the ground state at filling factors with even denominator, namely, $\nu = 1/2$ and $1/4$, by construction of $(l,m,q) = (3,3,1)$ and $(5,5,3)$ in Eq. (1), respectively.

The outline of the remainder of this paper is as follows. Section II introduces how to apply FHNC theory to the Halperin wave function, and introduces FHNC formalism to compute the radial distribution function. Section III is devoted to the results and the conclusions.

II. METHOD

As an application of the FHNC theory to the FQHE, we can rewrite HWF given by Eq. (1) as the Jastrow-Slater type wave function:

$$\Psi(\mathbf{R}^\uparrow,\mathbf{R}^\downarrow) = \prod_{i<j}^{N^\uparrow} f^{\uparrow\uparrow}(z_i,z_j) \prod_{i<j}^{N^\downarrow} f^{\downarrow\downarrow}(z_i,z_j) \times \prod_{i,j}^{N^\uparrow,N^\downarrow} f^{\uparrow\downarrow}(z_i,z_j)\Phi_0^\uparrow\Phi_0^\downarrow, \tag{5}$$

where spin-dependent dynamical correlation factors, $f^{\sigma\sigma'}(z_i,z_j) \equiv \exp[u^{\sigma\sigma'}(z_i,z_j)/2]$, are generated by pseudopotentials $u^{\sigma\sigma'}(z_i,z_j)$ given as $u^{\uparrow\uparrow}(z_i,z_j) = 2(l-1)\ln(z_i^\uparrow - z_j^\uparrow)$, $u^{\downarrow\downarrow}(z_i,z_j) = 2(m-1)\ln(z_i^\downarrow - z_j^\downarrow)$, and $u^{\uparrow\downarrow}(z_i,z_j) = 2q\ln(z_i^\uparrow - z_j^\downarrow)$. Slater (Vandermonde) determinants Φ_0^σ of renormalized single-electron wave functions, $\varphi_\alpha^\sigma = c_\alpha^\sigma z^\alpha \exp(-\pi\rho^\sigma|z|^2/2)$, with spin σ and a normalization constant c_α^σ, where $\alpha = 0,1,\ldots,N^\sigma - 1$, describe only the noninteracting system of spin σ electrons in the LLL. The density of the spin σ electron is $\rho^\sigma = \nu^\sigma/(2\pi\ell_0)$, which relates to the filling factor given by Eq. (2).

Since the HWF is completely in the LLL, the kinetic energy per particle is restricted to having the lowest cyclotron energy $\hbar\omega_c/2$, where $\omega_c = eB/cm^*$ is the cyclotron frequency, and m^* is the effective mass of the electron in the background. The spin-dependent Coulomb interaction between electrons is given by

$$V_C = \sum_{i<j}^{N^\uparrow} \frac{e^2}{\epsilon|z_i^\uparrow - z_j^\uparrow|} + \sum_{i<j}^{N^\downarrow} \frac{e^2}{\epsilon|z_i^\downarrow - z_j^\downarrow|} + \sum_{i,j}^{N^\uparrow,N^\downarrow} \frac{e^2}{\epsilon|z_i^\uparrow - z_j^\downarrow|}, \tag{6}$$

where ϵ is the dielectric constant of the background material. The interaction energy per particle for any given wave function is given by

$$\begin{aligned} E = \frac{\langle V_C + V_{ex}\rangle}{N} &= \frac{1}{2}\frac{(\rho^\uparrow)^2}{\rho}\int d\mathbf{r}[g^{\uparrow\uparrow}(r) - 1]v_c(r) \\ &+ \frac{1}{2}\frac{(\rho^\downarrow)^2}{\rho}\int d\mathbf{r}[g^{\downarrow\downarrow}(r) - 1]v_c(r) \\ &+ \frac{\rho^\uparrow\rho^\downarrow}{\rho}\int d\mathbf{r}[g^{\uparrow\downarrow}(r) - 1]v_c(r), \end{aligned} \tag{7}$$

where V_{ex} implies the interactions between electron and background ion and those among background ions, and $v_c(r) = e^2/\epsilon r$ with $r \equiv r_{ij} = |z_i - z_j|$. The spin-dependent radial distribution functions $g^{\sigma\sigma'}(r_{ij})$ are defined by

$$g^{\sigma\sigma}(r_{ij}) = \frac{N^\sigma(N^\sigma - 1)}{\rho^{\sigma 2}\langle\Psi|\Psi\rangle}\int d\mathbf{R}^{(z_i^\sigma,z_j^\sigma)}|\Psi(\mathbf{R}^\uparrow,\mathbf{R}^\downarrow)|^2, \tag{8}$$

$$g^{\uparrow\downarrow}(r_{ij}) = \frac{N^\uparrow N^\downarrow}{\rho^\uparrow\rho^\downarrow\langle\Psi|\Psi\rangle}\int d\mathbf{R}^{(z_i^\uparrow,z_j^\downarrow)}|\Psi(\mathbf{R}^\uparrow,\mathbf{R}^\downarrow)|^2, \tag{9}$$

with $\sigma\sigma = \uparrow\uparrow,\downarrow\downarrow$, where $d\mathbf{R}^{(z_1^\sigma,z_2^\sigma)}$ denotes the product of all volume elements, except $d^2z_i^\sigma$ and $d^2z_j^\sigma$, and ρ^σ is the spin σ electron density. The spin-dependent static structure functions $S^{\sigma\sigma'}(\mathbf{k})$ associated with the Fourier transform of radial distribution functions Eqs. (8) and (9) are defined as

$$S^{\sigma\sigma'}(\mathbf{k}) = \delta_{\sigma\sigma'} + \sqrt{\rho^\sigma\rho^{\sigma'}}\int d\mathbf{r}[g^{\sigma\sigma'}(r) - 1]e^{i\mathbf{k}\cdot\mathbf{r}}. \quad (10)$$

The spin-dependent single-particle density matrix of the system is defined by

$$n^\sigma\left(z_1^\sigma,z_1'^\sigma\right) = \frac{N^\sigma}{\langle\Psi|\Psi\rangle}\int d\mathbf{R}^{(z_1^\sigma,z_1'^\sigma)}\Psi^*\left(z_1^\sigma,z_2^\sigma,\cdots,z_{N^\sigma}^\sigma\right) \times \Psi\left(z_1'^\sigma,z_2^\sigma,\cdots,z_{N^\sigma}^\sigma\right). \quad (11)$$

In order to obtain the interaction energy of Eq. (7) we should find the spin-dependent radial distribution function $g^{\sigma\sigma}(r_{ij})$ through the application of FHNC theory. The integrand $|\Psi|^2$ in Eqs. (8) and (9) can be expanded in powers of the spin-dependent direct bond functions $h^{\sigma\sigma'}(r_{ij}) = [f^{\sigma\sigma'}(r_{ij})]^2 - 1$, which has the property of $h^{\sigma\sigma'}(r_{ij}) \to 0$, at $r_{ij} \to \infty$, as

$$|\Psi|^2 = \left\{1 + \sum_{\sigma\sigma'}\left[\sum_{i<j}^{N} h^{\sigma\sigma'}(r_{ij})\sum_{i<j}^{N}\sum_{k<l}^{N} h^{\sigma\sigma'}(r_{ij})h^{\sigma\sigma'}(r_{kl}) + \cdots\right]\right\}\left|\Phi_0^\sigma\right|^2\left|\Phi_0^{\sigma'}\right|^2. \quad (12)$$

We analytically determine the statistical exchange bond function, defined by $\ell^\sigma(z_i,z_j) = n_0^\sigma(z_i,z_j)/\rho^\sigma$, where $n_0^\sigma(z_i,z_j)$ is the uncorrelated one-body density matrix, from the Slater determinants $|\Phi_0^\sigma|^2$, $|\Phi_0^{\sigma'}|^2$ in the form

$$n_0^\sigma(z_i,z_j) = \sum_{\alpha=0}^{N^\sigma-1}\varphi^{*\sigma}_\alpha(z_i)\varphi_\alpha^\sigma(z_j). \quad (13)$$

In our case, the exchange bond function is explicitly determined as the form in the thermodynamic limit,

$$\ell^\sigma(z_i,z_j) = \exp\left(-\frac{\pi}{2}\rho^\sigma|z_i - z_j|^2\right) \times \exp[-i\pi\rho^\sigma r_i r_i \sin(\theta_i - \theta_j)], \quad (14)$$

where θ_i is given by $z_i = r_i\exp(i\theta_i)$. As a consequence, the spin-dependent radial distribution functions $g^{\sigma\sigma'}(r_{ij})$, given by Eqs. (8) and (9), are expressed as a sum of all irreducible cluster diagrams, which are constructed with both bond functions, $h^{\sigma\sigma'}(r_{ij})$ and $\ell^\sigma(z_i,z_j)$. All irreducible diagrams, obeying well-defined topological rules [38,39], are distinguished by three types of diagrams: nodal, non-nodal, and elementary diagrams. For each type of diagram there are four different classes, namely, dd (direct-direct), de (direct-exchange), ee (exchange-exchange), and cc (circular-circular) for each spin configuration $\sigma\sigma' = \uparrow\uparrow,\uparrow\downarrow,\downarrow\uparrow,\downarrow\downarrow$.

The sums of spin-dependent non-nodal (diagrams) functions of the four types are given by

$$X_{dd}^{\sigma\sigma'}(r) = \Gamma_{dd}^{\sigma\sigma'}(r) - N_{dd}^{\sigma\sigma'}(r) - 1, \quad (15)$$

$$X_{de}^{\sigma\sigma'}(r) = \Gamma_{dd}^{\sigma\sigma'}(r)\left[N_{de}^{\sigma\sigma'}(r) + E_{de}^{\sigma\sigma'}(r)\right] - N_{de}^{\sigma\sigma'}(r), \quad (16)$$

$$X_{ee}^{\sigma\sigma'}(r) = \Gamma_{dd}^{\sigma\sigma'}(r)\left\{N_{ee}^{\sigma\sigma'}(r) + E_{ee}^{\sigma\sigma'}(r) + \left[N_{de}^{\sigma\sigma'}(r) + E_{ee}^{\sigma\sigma'}(r)\right]^2\right\} - \delta_{\sigma\sigma'}\Gamma_{dd}^{\sigma\sigma'}(r)\left[N_{cc}^{\sigma\sigma'}(r) + E_{cc}^{\sigma\sigma'}(r) - \ell^\sigma\right]^2 - N_{ee}^{\sigma\sigma'}(r), \quad (17)$$

$$X_{cc}^{\sigma\sigma}(r) = \Gamma_{dd}^{\sigma\sigma}(r)\left[N_{cc}^{\sigma\sigma}(r) + E_{cc}^{\sigma\sigma}(r)\right] + \left[1 - \Gamma_{dd}^{\sigma\sigma}(r)\right]\ell^\sigma - N_{cc}^{\sigma\sigma}(r) - 1, \quad (18)$$

with

$$\Gamma_{dd}^{\sigma\sigma'}(r) = \exp\left[u^{\sigma\sigma'}(r) + N_{dd}^{\sigma\sigma'}(r) + E_{dd}^{\sigma\sigma'}(r)\right]. \quad (19)$$

The class of spin-dependent nodal (diagrams) functions is given by convolution equations in the form

$$N_{dd}^{\sigma\sigma'}(r_{12}) = \sum_{\sigma_3}\rho^{\sigma_3}\int dr_3\left[X_{dd}^{\sigma\sigma_3}(r_{13}) + X_{de}^{\sigma\sigma_3}(r_{13})\right]\left[N_{dd}^{\sigma_3\sigma'}(r_{32}) + X_{dd}^{\sigma_3\sigma'}(r_{32})\right] + \sum_{\sigma_3}\rho^{\sigma_3}\int dr_3 X_{dd}^{\sigma\sigma_3}(r_{13})\left[N_{ed}^{\sigma_3\sigma'}(r_{32}) + X_{ed}^{\sigma_3\sigma'}(r_{32})\right], \quad (20)$$

$$N_{de}^{\sigma\sigma'}(r_{12}) = \sum_{\sigma_3}\rho^{\sigma_3}\int dr_3\left[X_{dd}^{\sigma\sigma_3}(r_{13}) + X_{de}^{\sigma\sigma_3}(r_{13})\right]\left[N_{de}^{\sigma_3\sigma'}(r_{32}) + X_{de}^{\sigma_3\sigma'}(r_{32})\right] + \sum_{\sigma_3}\rho^{\sigma_3}\int dr_3 X_{dd}^{\sigma\sigma_3}(r_{13})\left[N_{ee}^{\sigma_3\sigma'}(r_{32}) + X_{ee}^{\sigma_3\sigma'}(r_{32})\right], \quad (21)$$

$$N_{ee}^{\sigma\sigma'}(r_{12}) = \sum_{\sigma_3}\rho^{\sigma_3}\int dr_3\left[X_{ed}^{\sigma\sigma_3}(r_{13}) + X_{ee}^{\sigma\sigma_3}(r_{13})\right]\left[N_{de}^{\sigma_3\sigma'}(r_{32}) + X_{de}^{\sigma_3\sigma'}(r_{32})\right] + \sum_{\sigma_3}\rho^{\sigma_3}\int dr_3 X_{ed}^{\sigma\sigma_3}(r_{13})\left[N_{ee}^{\sigma_3\sigma'}(r_{32}) + X_{ee}^{\sigma_3\sigma'}(r_{32})\right], \quad (22)$$

$$N_{cc}^{\sigma\sigma}(r_{12}) = \sum_{\sigma}\rho^{\sigma}\int dr_3 X_{cc}^{\sigma\sigma}(r_{13})\left[N_{cc}^{\sigma\sigma}(r_{32}) + X_{cc}^{\sigma\sigma}(r_{32})\right] + \sum_{\sigma}\rho^{\sigma}\int dr_3 X_{cc}^{\sigma\sigma}(r_{13})\ell^\sigma(r_{32}). \quad (23)$$

The spin-dependent radial distribution function is composed of the components

$$g^{\sigma\sigma'}(r) = 1 + \sum_{\alpha\beta}\left[X^{\sigma\sigma'}_{\alpha\beta}(r) + N^{\sigma\sigma'}_{\alpha\beta}(r)\right], \tag{24}$$

where $\alpha\beta$ denotes dd,de,ed, and ee.

All spin-dependent nodal functions, except $N^{\sigma\sigma}_{cc}(r_{12})$, can be factorized in the reciprocal spaces through the Fourier transformations of Eqs. (20)–(22). We determine the explicit expression for spin-dependent nodal functions in the reciprocal space after some algebra, which we show in the Appendix. They are useful tools in an iteration procedure for the numerical calculation. In general, due to the phase factor of the exchange bond function, implied in cc nodal functions, the spin-dependent $N^{\sigma\sigma'}_{cc}$ of Eq. (23) must be solved by using a multidimensional integration.

The FHNC equations provide a closed set of equations for the nodal functions in the reciprocal space represented in the Appendix, and additionally in Eqs. (23) and the non-nodal functions in Eqs. (15)–(19), only if the elementary diagrams $E^{\sigma\sigma'}_{\alpha\beta}$ are known. For simplicity, we can neglect all elementary diagrams, a so-called FHNC//0 approximation. In the numerical calculation pseudopotentials $u^{\sigma\sigma}(r)$ can be divided into short-range and long-range parts, namely, $u^{\sigma\sigma}(r) = u^{\sigma\sigma}_s(r) + u^{\sigma\sigma}_l(r)$.

In our case, we can separate the pseudopotential $u^{\uparrow\uparrow}(r) = 2(l-1)\ln r$ into $u^{\uparrow\uparrow}_s(r) = -2(l-1)K_0(Qr)$ and $u^{\uparrow\uparrow}_l(r) = 2(l-1)[\ln r + K_0(Qr)]$, where $K_0(Qr)$ is the modified Bessel function and Q is a cutoff parameter of the order of unity. Since $K_0(Qr) = -\ln(Qr/2) - \gamma$ as $r \to 0$, where $\gamma = 0.5772\cdots$ is the Euler constant, $u^{\uparrow\uparrow}_l(0) = -2(l-1)\gamma$, $u^{\downarrow\downarrow}_l(0) = -2(m-1)\gamma$, and $u^{\uparrow\downarrow}_l(0) = -2q\gamma$ at $r = 0$.

III. RESULTS AND DISCUSSION

We adopted a system of strongly correlated fermions with different spin degrees of freedom which may be represented by the HWF of Eq. (1), and applied the FHNC theory to study the spin-polarization effects in higher-order FQHE states at filling factors $\nu = 2/5, 3/8, 5/13, 4/11$, and $5/17$, located in the filling factor regime $2/3 > \nu > 2/7$, reported in the experimental results of Ref. [24]. We report numerical results on the ground-state interaction energy per particle, given by Eq. (7), through calculation of spin-dependent radial distribution functions, $g^{\sigma\sigma'}(r)$, at various filling factors in this range, by a FHNC//0 approximation in which all elementary diagrams are neglected on the cluster expansion.

Figure 1 compares $g^{\sigma\sigma'}_\nu(x)$, expressed by Eqs. (8) and (9), at filling factors $\nu = 4/11$ (black lines) and $3/7$ (blue lines), as functions of dimensionless variable $x = \sqrt{\nu/2}r/\ell_0$. Here, $g^{\uparrow\uparrow}_\nu(x)$ are denoted with solid lines, $g^{\uparrow\downarrow}_\nu(x)$ with dashed lines, and $g^{\downarrow\downarrow}_\nu(x)$ with dotted lines. They are quantities proportional to the probability of finding two electrons of spins σ and σ' at distance x. This shows that while filling factors vary in accord with the varied spin ratio in the LLL the peak positions of $g^{\sigma\sigma'}_\nu(x)$ for electrons with unlike spins and those with the same spin move in different directions. The LLLs at filling factors $\nu = 4/11$ and $3/7$, represented by the HWF with $(l,m,q) = (3,5,2)$ and $(3,5,1)$, respectively, possess spin polarizations $\zeta = 1/2$ ($\nu^\uparrow = 3/11$ and $\nu^\downarrow = 1/11$) and $1/3$ ($\nu^\uparrow = 2/7$ and $\nu^\downarrow = 1/7$) according to Eqs. (3) and (4). For both filling factors, $g^{\uparrow\downarrow}_\nu(x)$ obviously shows the characteristics of liquid states, and has a more pronounced peak than $g^{\sigma\sigma}_\nu(x)$, i.e., electrons with unlike spins correlate better than those with the same spin. Figure 2 shows the spin-polarization dependence of $g^{\sigma\sigma'}_\nu(x)$ at filling factor $\nu = 4/11$. According to increasing spin polarizations from $\zeta = 1/2$ to $3/4$ at filling factor $\nu = 4/11$, which correspond to $(l,m,q) = (3,5,2)$ and $(3,15,1)$ in the HWF, respectively, i.e., varying the spin

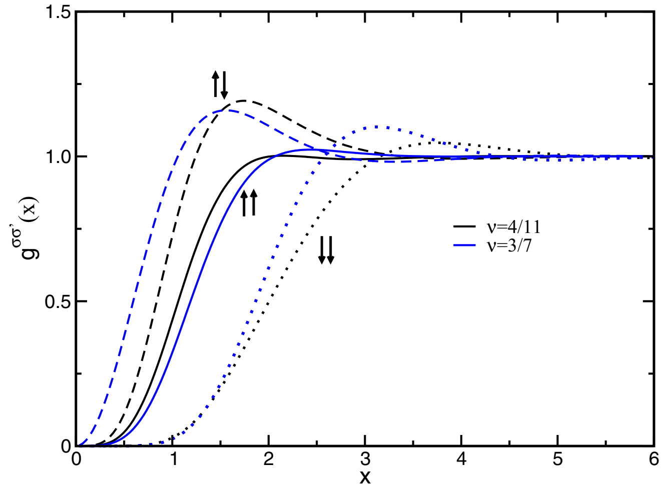

FIG. 1. Spin-dependent radial distribution functions $g^{\sigma\sigma'}(x)$ for filling factors $\nu = 4/11$ (black lines) and $3/7$ (blue lines) as a function of dimensionless variable $x = \sqrt{\nu/2}r/\ell_0$, for spin polarizations $\zeta = 1/2$ ($\nu^\uparrow = 3/11$ and $\nu^\downarrow = 1/11$) and $1/3$ ($\nu^\uparrow = 2/7$ and $\nu^\downarrow = 1/7$), respectively, calculated with the HWF by FHNC//0 approximation. $g^{\uparrow\uparrow}(x)$ at both filling factors are shown by solid lines, $g^{\uparrow\downarrow}(x)$ by dashed lines, and $g^{\downarrow\downarrow}(x)$ by dotted lines.

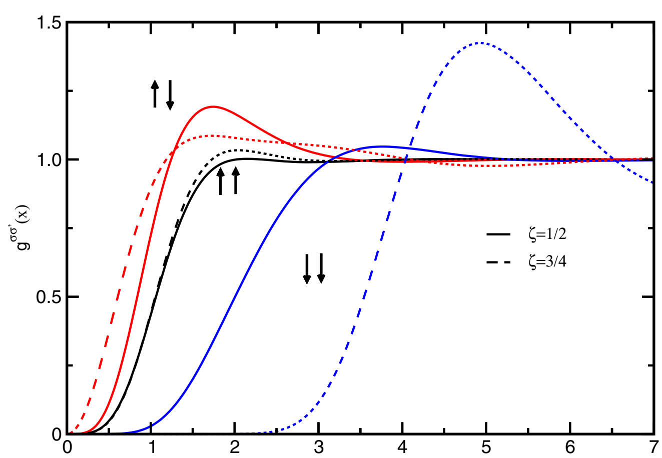

FIG. 2. Spin-dependent radial distribution functions $g^{\sigma\sigma'}(x)$ for spin polarization $\zeta = 1/2$ (solid lines) and $3/4$ (dashed lines) at a filling factor $\nu = 4/11$, as a function of dimensionless variable $x = \sqrt{\nu/2}r/\ell_0$. $g^{\uparrow\uparrow}(x)$ in terms of spin polarizations are denoted by black lines, $g^{\uparrow\downarrow}(x)$ by red lines, and $g^{\downarrow\downarrow}(x)$ by blue lines. $g^{\downarrow\downarrow}(x)$ is changed drastically by varying of the spin concentrations from $\eta^\downarrow = 1/4$ to $1/8$.

concentration, defined by $\eta^{\sigma} = N^{\sigma}/N$, from $\eta^{\downarrow} = 1/4$ to $1/8$, $g_{\nu}^{\downarrow\downarrow}(x)$ (blue lines) change drastically.

We find the interaction energy per particle of the FQH state in terms of spin polarizations at filling factor $\nu = 4/11$, related closely to $g_{\nu}^{\sigma\sigma'}(x)$ through Eq. (7), to be $E_{\nu}(\zeta) = -0.41297$ in units of $e^2/\epsilon\ell_0$ for $\zeta = 1/2$, and $E_{\nu}(\zeta) = -0.40364$ $(e^2/\epsilon\ell_0)$ for $\zeta = 3/4$. As a comparison, decrease of spin polarizations from $\zeta = 3/4$ to $1/2$ with respect to increase of spin-down concentrations from $\eta^{\downarrow} = 1/8$ to $1/4$ causes a reduction in the ground-state energy of the system with the value of $\Delta E_{\nu} = 0.0093(e^2/\epsilon\ell_0)$, which is the energy required to flip the spin of one electron, and this energy must be equal to the Zeeman energy, in order for the partially spin-polarized state at $\nu = 4/11$ for $\zeta = 1/2$ to be possible. We evaluate the Zeeman energy per particle from $E_Z = (1 - 2\eta^{\uparrow})sg\mu_B$, where $\eta^{\uparrow}$ is the ratio of the number of spins parallel to the magnetic field to the total number of spins, $\mu_B = e\hbar/2m_e c$ is the Bohr magneton, and $s = 1/2$, from Ref. [2]. For GaAs parameters (the Landé g factor $g = -0.44$ and $\epsilon = 13.6$) $E_Z \simeq 0.0093(e^2/\epsilon\ell_0)$ for $B \simeq 16$ T, where $\eta^{\uparrow} = 7/8$ in terms of the $4/11$ state for $\zeta = 3/4$.

Our results are in reasonable agreement with the estimates $E_{\nu}(\zeta) = -0.42054$ $(e^2/\epsilon\ell_0)$ by Chang *et al.* [36] at $\nu = 4/11$ for $\zeta = 1/2$, proposed with a diagonalization method of the CF basis wave function of a rather large system with respect to residual interactions between CFs in spherical geometry through a Monte Carlo method. Applying the FHNC//4 approximation, in which only four particle elementary diagrams are additionally considered in the FHNC theory, we can obtain quantitatively better results than when those are ignored, but in this paper we have not done so. The work of Park and Jain [40] with mixed states of CF carrying two and four vortices has also shown that the FQHE state at filling $\nu = 4/11$ is partially spin polarized or unpolarized. It is not clear whether the $\nu = 4/11$ state observed in a tilted magnetic field by Pan *et al.* [24] is fully polarized or not. However, it is quite possible that the state is fully polarized, since it is observed in high magnetic fields. This issue has been investigated theoretically by Jain's group [36]. Mukherjee *et al.* [41] have shown that a special kind of correlation between CFs in their partially filled effective Landau level is responsible for fully spin-polarized FQHE states in $\nu = 4/11$ and $5/13$.

Due to the restricted structure of HWF, we cannot here treat the ground-state energy of the fully spin-polarized state at $\nu = 4/11$. However, we might predict the ground-state energy of $E_{4/11}(1) \simeq -0.3912(e^2/\epsilon\ell_0)$ through using the relation of the Zeeman energy as $\eta^{\downarrow} \to 0$ at $\nu = 4/11$. This counts more than the estimates of $E_{4/11}(1) \simeq -0.4219(e^2/\epsilon\ell_0)$ for a system of four electrons by Chakraborty [2], and $E_{4/11}(1) = -0.41412(e^2/\epsilon\ell_0)$ by Chang *et al.* [36]. Such a discrepancy is due to the unsuitable HWF chosen for the full spin polarization at $\nu = 4/11$. Therefore, we restrict the HWF to study the spin polarization in between primary FQHE states, according to Eqs. (2)–(4). In accordance with our approach, the $3/7$ filling state, belonging to the primary FQHE sequences, is also partially spin polarized with $\zeta = 1/3$. Experimental evidence for this filling state has been provided in the luminescence spectra measurement by Kukushkin *et al.* [20].

Table I presents our results on the ground-state energy per particle at various filling factors with spin polarizations in higher-order FQH states, lying in between primary FQHE states. Table I also shows the dependence of ground-state energies on partial and full spin polarizations at the same filling factor. The result on the ground-state energy at $\nu = 4/11$ for $\zeta = 1/2$ by FHNC//0 approximation is in good agreement within a few percent with that of Chang and Jain [36]. The interaction energy per particle at filling factor $\nu = 3/8$ with respect to spin polarization $\zeta = 2/3$ is $E_{3/8}(2/3) = -0.40735(e^2/\epsilon\ell_0)$.

The static structure function, defined by Eq. (10), is related to the radial distribution function by Fourier transform. The two quantities appeal to different intuitions. For completeness, in Fig. 3, we plot spin-dependent static structure functions $S^{\sigma\sigma}(q)$ at various filling factors $\nu = 4/11$ (black lines) and

TABLE I. Ground-state energy per particle $E_{\nu}(\zeta)$ in units of $e^2/\epsilon\ell_0$ at various filling factors, $\nu = \frac{2}{9}, \frac{3}{7}, \frac{2}{5}, \frac{2}{7}, \frac{3}{8}, \frac{4}{11}, \frac{5}{13}, \frac{5}{17}$, and $\frac{6}{17}$, where ζ is the spin polarization. The first column indicates the filling factors of the ground states. The second column displays our results by FHNC//0 approximation, using the HWF for the spin polarizations at various filling states in the thermodynamic limits. We compare them in the third and fourth columns with the estimates of Jain and Kamilla for full spin polarization [42], by using projected CF wave functions in the spherical geometry, results of Morf *et al.* by Monte Carlo method [43], the estimates of Dharma-Wardana [44], and more. References [36,41,45–47] have used the CF-diagonalization method.

ν	$E_{\nu}(\zeta)$		
$\frac{2}{9}$	$E_{\nu}(0) = -0.33830$	$E_{\nu}(1) = -0.3428$ [42]	$E_{\nu}(1) = -0.340$[44]
	$E_{\nu}(1/2) = -0.33514$		
$\frac{3}{7}$	$E_{\nu}(1/3) = -0.42724$	$E_{\nu}(1) = -0.44228$ [42]	$E_{\nu}(1) = -0.445$ [44]
$\frac{2}{5}$	$E_{\nu}(0) = -0.43345$	$E_{\nu}(1) = -0.43280$ [42]	$E_{\nu}(1) = -0.4142$ [43]
	$E_{\nu}(1/2) = -0.41601$		
$\frac{2}{7}$	$E_{\nu}(0) = -0.36925$	$E_{\nu}(1) = -0.3773$ [43]	
$\frac{3}{8}$	$E_{\nu}(2/3) = -0.40735$	$E_{\nu}(1/3) = -0.4256$ [45]	$E_{\nu}(1) = -0.41952$ [45]
$\frac{4}{11}$	$E_{\nu}(1/2) = -0.41297$		$E_{\nu}(1/2) = -0.4219$ [36]
	$E_{\nu}(3/4) = -0.40364$		$E_{\nu}(1) = -0.41412$ [36,41]
$\frac{5}{13}$	$E_{\nu}(3/5) = -0.41058$		$E_{\nu}(1) = -0.42431$ [41]
$\frac{5}{17}$	$E_{\nu}(1/5) = -0.35781$		$E_{\nu}(1) = -0.38591$ [46]
$\frac{6}{17}$	$E_{\nu}(2/3) = -0.40756$		$E_{\nu}(1) = -0.41228$ [47]

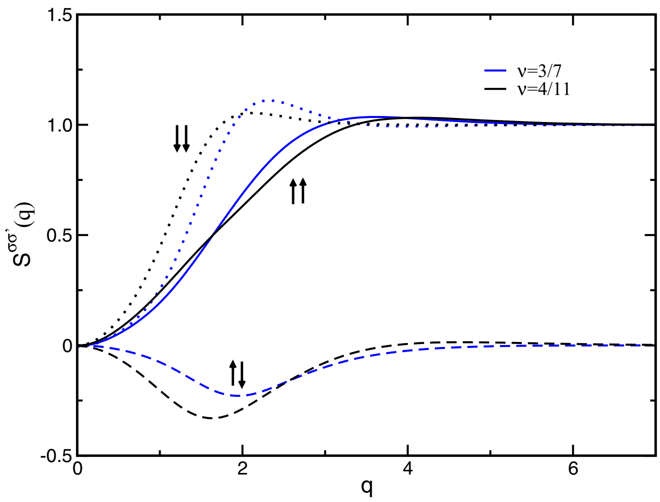

FIG. 3. Spin-dependent static structure functions $S^{\sigma\sigma'}(q)$ for $\nu = 4/11$ (black lines) and 3/7 (blue lines) as a function of $q = \sqrt{2/\nu}k\ell_0$, obtained from the HWF by FHNC//0. $S^{\uparrow\uparrow}(q)$ for different filling factors are shown by solid lines, $S^{\uparrow\downarrow}(q)$ by dashed lines, and $S^{\downarrow\downarrow}(q)$ by dotted lines.

3/7 (blue lines), as a function of the dimensionless variable $q = \sqrt{2/\nu}k\ell_0$.

In addition, we obtain results for the FQHE states at even-denominator fractions, $\nu = 1/2$ and 1/4, represented by the HWF of $(l,m,q) = (3,3,1)$ and $(5,5,3)$, in Eq. (1), respectively, with respect to the spin polarization of a model system. Neither of them are spin polarized by Eq. (4). In Fig. 4, we plot $g^{\sigma\sigma'}(x)$ at filling factors $\nu = 1/2$ (black line) and 1/4 (red lines) as a function of x, where $g^{\sigma\sigma}(x)$ is depicted by solid lines, and $g^{\uparrow\downarrow}(x)$ by dashed lines. Figure 4 shows that $g^{\uparrow\downarrow}(x)$ at even-denominator filling states also has a pronounced peak, as likely shown in Figs. 1 and 2, whereas $g^{\sigma\sigma}(x)$ at both filling factors displays the characteristic of a system of weakly correlated particles, as a free-electron gas. This means that the pair correlations between unlike spins dominate at even-denominator filling factors. In Table II, we report the ground-state energies at even-denominator fillings for the unpolarized spin, compared with results for the fully spin-polarized even-denominator fillings, which are referred to in Refs. [37,48,49]. There are small discrepancies among them. However, in the $\nu = 1/2$ case, our result $E_{1/2}(0) = -0.4567(e^2/\epsilon\ell_0)$ falls within the error bar of $E_{1/2}(1)$ obtained by others. Therefore we cannot tell which state is more favorable between the fully polarized state and the unpolarized one.

TABLE II. Ground-state energy per particle $E(\nu)$ in units of $e^2/\epsilon\ell_0$ at filling factors of even denominators, $\nu = \frac{1}{2}$ and $\frac{1}{4}$. The second column displays our results employed with the HWF by FHNC//0 approximation.

ν	$E_\nu(\zeta)$	References
$\frac{1}{2}$	$E_\nu(0) = -0.4567$	$E_\nu(1) = -0.425$ [37]
		$E_\nu(1) = -0.469$ [49]
		$E_\nu(1) = -0.479$ [48]
$\frac{1}{4}$	$E_\nu(0) = -0.3542$	$E_\nu(1) = -0.3624$ [48]

Finally, in Fig. 5 we plot the spin-dependent $S^{\sigma\sigma'}(x)$ for the filling factors $\nu = 1/2$ (black lines) and 1/4 (red lines) as a function of the dimensionless variable $q = \sqrt{2/\nu}k\ell_0$. Solid lines indicate $S^{\uparrow\uparrow}(q)$ for both filling factors, and dashed lines indicate $S^{\uparrow\downarrow}(q)$. Figure 5 also shows that $S^{\sigma\sigma}(x)$ are almost the same at both of the filling factors, in contrast to $S^{\uparrow\downarrow}(x)$.

IV. CONCLUSIONS

Using the Halperin wave function to represent the partially spin-polarized states of a system of strongly correlated fermions with the spin degree of freedom at the lowest Landau level, we have calculated the radial distribution functions and

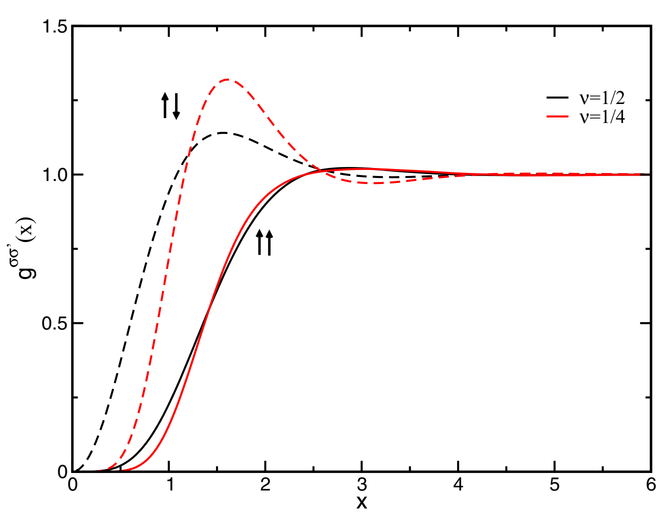

FIG. 4. Spin-dependent radial distribution function $S^{\sigma\sigma'}(x)$ for the filling factors $\nu = 1/2$ (black lines) and 1/4 (red lines) as a function of dimensionless $x = \sqrt{\nu/2}r/\ell_0$, obtained from the HWF by FHNC//0. Solid lines indicate $g^{\uparrow\uparrow}(x) = g^{\downarrow\downarrow}(x)$ for both filling factors, and dashed lines indicate $g^{\uparrow\downarrow}(x)$.

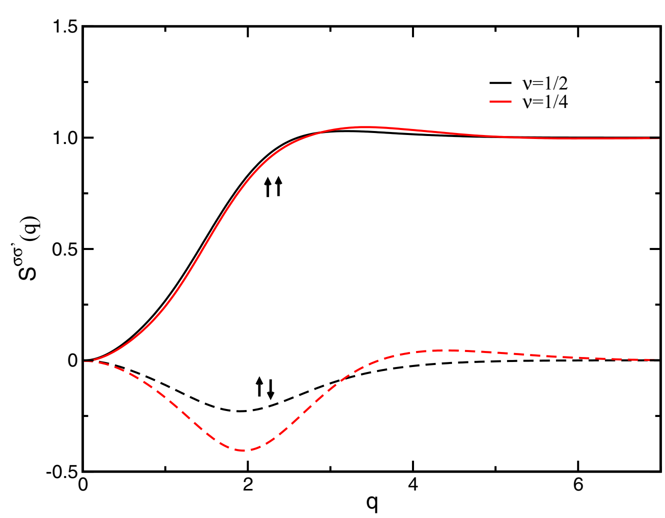

FIG. 5. Spin-dependent static structure functions $S^{\sigma\sigma'}(x)$ for the filling factors $\nu = 1/2$ (black lines) and 1/4 (red lines) as a function of dimensionless variable $q = \sqrt{2/\nu}k\ell_0$, employed with the HWF by FHNC//0 approximation. Solid lines indicate $S^{\uparrow\uparrow}(q)$ for both filling factors, and dashed lines indicate $S^{\uparrow\downarrow}(q)$.

the static structure functions through application of the Fermi hypernetted-chain theory in order to study the spin polarization of the fractional quantum Hall effect at a filling factor range of $2/3 > \nu > 2/7$, and of even-denominator fractions. Our result for the ground-state energy at the filling factor $\nu = 4/11$ with the spin polarization of $\zeta = 1/2$ is in agreement with the estimates by Chang and Jain, proposed with a diagonalization method of the composite fermion basis wave function of a rather large system with respect to residual interactions between composite fermions in spherical geometry through a Monte Carlo method. Our future aim would be using the FHNC theory to study a system of fermions with spin and Dirac-valley degrees of freedom such as graphene. Such a system has been already well studied by others, for instance, by Modak *et al.* [50] using Chern-Simons theory. Note that our formalism deals with a system which can be described by the Halperin wave function. The FHNC theory provides not only ground-state energy but also detailed information about the pair-correlation functions, which give us better understanding on the stability of the states.

ACKNOWLEDGMENTS

This research was supported by the Basic Science Research Program through the National Research Foundation of Korea, funded by the Ministry of Education, Science and Technology (Grants No. NRF-2015R 1D 1A 1A01058031 and No. NRF-2012R1A1A2006303).

APPENDIX: SPIN-DEPENDENT NODAL FUNCTIONS IN THE RECIPROCAL SPACE

The class of spin-dependent nodal functions $N_{\alpha\beta}^{\sigma\sigma'}$ (with $\alpha\beta = dd,de,ed,ee$), given by Eqs. (20)–(22), can be solved explicitly in the reciprocal space as the following forms:

$$N_{dd}^{\uparrow\uparrow}(k) = -X_{dd}^{\uparrow\uparrow}(k) + \frac{1}{P(k)} \times \{a_1 X_{dd}^{\downarrow\uparrow}(k) - b_1 X_{dd}^{\uparrow\uparrow}(k) - \delta_1[N_{ed}^{\uparrow\uparrow}(k) + X_{ed}^{\uparrow\uparrow}(k)] - \delta_2[N_{ed}^{\downarrow\uparrow}(k) + X_{ed}^{\downarrow\uparrow}(k)]\}, \tag{A1}$$

$$N_{dd}^{\uparrow\downarrow}(k) = -X_{dd}^{\uparrow\downarrow}(k) + \frac{1}{P(k)} \times \{a_1 X_{dd}^{\downarrow\uparrow}(k) - b_1 X_{dd}^{\uparrow\downarrow}(k) - \delta_1[N_{ed}^{\uparrow\downarrow}(k) + X_{ed}^{\uparrow\downarrow}(k)] - \delta_2[N_{ed}^{\downarrow\downarrow}(k) + X_{ed}^{\downarrow\downarrow}(k)]\}, \tag{A2}$$

$$N_{dd}^{\downarrow\uparrow}(k) = -X_{dd}^{\downarrow\uparrow}(k) + \frac{1}{P(k)} \times \{b_2 X_{dd}^{\uparrow\uparrow}(k) - a_2 X_{dd}^{\downarrow\uparrow}(k) - \beta_1[N_{ed}^{\uparrow\uparrow}(k) + X_{ed}^{\uparrow\uparrow}(k)] - \beta_2[N_{ed}^{\downarrow\uparrow}(k) + X_{ed}^{\downarrow\uparrow}(k)]\}, \tag{A3}$$

$$N_{dd}^{\downarrow\downarrow}(k) = -X_{dd}^{\downarrow\downarrow}(k) + \frac{1}{P(k)} \times \{b_2 X_{dd}^{\uparrow\downarrow}(k) - a_2 X_{dd}^{\downarrow\downarrow}(k) - \beta_1[N_{ed}^{\uparrow\downarrow}(k) + X_{ed}^{\uparrow\downarrow}(k)] - \beta_2[N_{ed}^{\downarrow\downarrow}(k) + X_{ed}^{\downarrow\downarrow}(k)]\}, \tag{A4}$$

with

$$a_1 = -\frac{\rho^{\downarrow}}{\rho}[X_{dd}^{\uparrow\downarrow}(k) + X_{de}^{\uparrow\downarrow}(k)],$$
$$a_2 = 1 - \frac{\rho^{\uparrow}}{\rho}[X_{dd}^{\uparrow\uparrow}(k) + X_{de}^{\uparrow\uparrow}(k)], \tag{A5}$$

$$b_1 = 1 - \frac{\rho^{\downarrow}}{\rho}[X_{dd}^{\downarrow\downarrow}(k) + X_{de}^{\downarrow\downarrow}(k)],$$
$$b_2 = -\frac{\rho^{\uparrow}}{\rho}[X_{dd}^{\downarrow\uparrow}(k) + X_{de}^{\downarrow\uparrow}(k)], \tag{A6}$$

$$\beta_1 = \frac{\rho^{\uparrow}}{\rho}[a_1 X_{dd}^{\downarrow\uparrow}(k) - b_2 X_{dd}^{\uparrow\uparrow}(k)],$$
$$\beta_2 = \frac{\rho^{\downarrow}}{\rho}[a_1 X_{dd}^{\downarrow\downarrow}(k) - b_2 X_{dd}^{\uparrow\downarrow}(k)], \tag{A7}$$

$$\delta_1 = \frac{\rho^{\uparrow}}{\rho}[b_1 X_{dd}^{\uparrow\uparrow}(k) - a_2 X_{dd}^{\downarrow\uparrow}(k)],$$
$$\delta_2 = \frac{\rho^{\downarrow}}{\rho}[b_1 X_{dd}^{\uparrow\downarrow}(k) - a_2 X_{dd}^{\downarrow\downarrow}(k)], \tag{A8}$$

where the denominator $P(k)$ is defined as $P(k) = a_1 b_2 - a_2 b_1$. The de-nodal functions in the reciprocal coordinates are given by

$$N_{de}^{\uparrow\uparrow}(k) = -X_{de}^{\uparrow\uparrow}(k) + \frac{1}{P(k)} \times \{a_1 X_{de}^{\downarrow\uparrow}(k) - b_1 X_{de}^{\uparrow\uparrow}(k) - \delta_1[N_{ee}^{\uparrow\uparrow}(k) + X_{ee}^{\uparrow\uparrow}(k)] - \delta_2[N_{ee}^{\downarrow\uparrow}(k) + X_{ee}^{\downarrow\uparrow}(k)]\}, \tag{A9}$$

$$N_{de}^{\uparrow\downarrow}(k) = -X_{de}^{\uparrow\downarrow}(k) + \frac{1}{P(k)} \times \{a_1 X_{de}^{\downarrow\downarrow}(k) - b_1 X_{de}^{\uparrow\downarrow}(k) - \delta_1[N_{ee}^{\uparrow\downarrow}(k) + X_{ee}^{\uparrow\downarrow}(k)] - \delta_2[N_{ee}^{\downarrow\downarrow}(k) + X_{ee}^{\downarrow\downarrow}(k)]\}, \tag{A10}$$

$$N_{de}^{\downarrow\uparrow}(k) = -X_{de}^{\downarrow\uparrow}(k) + \frac{1}{P(k)} \times \{b_2 X_{de}^{\uparrow\uparrow}(k) - a_2 X_{de}^{\downarrow\uparrow}(k) - \beta_1[N_{ee}^{\uparrow\uparrow}(k) + X_{ee}^{\uparrow\uparrow}(k)] - \beta_2[N_{ee}^{\downarrow\uparrow}(k) + X_{ee}^{\downarrow\uparrow}(k)]\}, \tag{A11}$$

$$N_{de}^{\downarrow\downarrow}(k) = -X_{de}^{\downarrow\downarrow}(k) + \frac{1}{P(k)} \times \{b_2 X_{de}^{\uparrow\downarrow}(k) - a_2 X_{de}^{\downarrow\downarrow}(k) - \beta_1[N_{ee}^{\uparrow\downarrow}(k) + X_{ee}^{\uparrow\downarrow}(k)] - \beta_2[N_{ee}^{\downarrow\downarrow}(k) + X_{ee}^{\downarrow\downarrow}(k)]\}. \tag{A12}$$

Furthermore, the ee-nodal functions $N_{ee}^{\sigma\sigma'}(k)(\sigma\sigma' = \uparrow\uparrow,\uparrow\downarrow,\downarrow\uparrow,\downarrow\downarrow)$ can be expressed only with non-nodal functions $X_{\alpha\beta}^{\sigma\sigma'}$ in the form

$$N_{ee}^{\uparrow\uparrow}(k) = -X_{ee}^{\uparrow\uparrow}(k) + \frac{1}{D(k)}[-\mathcal{L}_4 X_{ee}^{\uparrow\downarrow}(k) + R_1 X_{de}^{\uparrow\uparrow}(k) + R_2 X_{de}^{\uparrow\downarrow}(k) + R_3 X_{ee}^{\uparrow\uparrow}(k)], \tag{A13}$$

$$N_{ee}^{\uparrow\downarrow}(k) = -X_{ee}^{\uparrow\downarrow}(k) + \frac{1}{D(k)}[-\mathcal{L}_4 X_{ee}^{\downarrow\downarrow}(k) + R_1 X_{de}^{\uparrow\downarrow}(k) + R_2 X_{de}^{\downarrow\downarrow}(k) + R_3 X_{ee}^{\uparrow\downarrow}(k)], \tag{A14}$$

$$N_{ee}^{\downarrow\uparrow}(k) = -X_{ee}^{\downarrow\uparrow}(k) + \frac{1}{D(k)}\big[-\mathcal{L}_1 X_{ee}^{\downarrow\uparrow}(k) + C_1 X_{de}^{\uparrow\uparrow}(k) + C_2 X_{de}^{\uparrow\downarrow}(k) + C_3 X_{ee}^{\uparrow\uparrow}(k)\big], \tag{A15}$$

$$N_{ee}^{\downarrow\downarrow}(k) = -X_{ee}^{\downarrow\downarrow}(k) + \frac{1}{D(k)}\big[-\mathcal{L}_1 X_{ee}^{\downarrow\downarrow}(k) + C_1 X_{de}^{\uparrow\downarrow}(k) + C_2 X_{de}^{\downarrow\downarrow}(k) + C_3 X_{ee}^{\uparrow\downarrow}(k)\big], \tag{A16}$$

where $D(k)$ is given as follows:

$$D(k) = \frac{\rho^\uparrow}{\rho}\mathcal{L}_2\big[X_{de}^{\downarrow\uparrow}(k) + X_{ee}^{\downarrow\uparrow}(k)\big] + \frac{\rho^\uparrow}{\rho}\mathcal{L}_4 X_{de}^{\downarrow\uparrow}(k) - \frac{\rho^\downarrow}{\rho}\mathcal{L}_3\big[X_{de}^{\downarrow\downarrow}(k) + X_{ee}^{\downarrow\downarrow}(k)\big] - \mathcal{L}_1\left[1 - \frac{\rho^\downarrow}{\rho}X_{de}^{\downarrow\downarrow}(k)\right], \tag{A17}$$

and

$$\mathcal{L}_1 = P(k)\left[1 - \frac{\rho^\uparrow}{\rho}X_{ed}^{\uparrow\uparrow}(k)\right] + \frac{\rho^\uparrow}{\rho}\delta_1\big[X_{ed}^{\uparrow\uparrow}(k) - X_{ee}^{\uparrow\uparrow}(k)\big] + \frac{\rho^\downarrow}{\rho}\beta_1[X_{ed}^{\uparrow\downarrow}(k) - X_{ee}^{\uparrow\downarrow}(k)], \tag{A18}$$

$$\mathcal{L}_2 = \delta_2\left[1 - \frac{\rho^\uparrow}{\rho}X_{ed}^{\uparrow\uparrow}(k)\right] - \frac{\rho^\uparrow\rho^{\downarrow 2}}{\rho^3}\big[X_{dd}^{\uparrow\downarrow}(k)X_{dd}^{\downarrow\uparrow}(k) + X_{dd}^{\uparrow\uparrow}(k)X_{dd}^{\downarrow\downarrow}(k)\big] \times\big[X_{ed}^{\uparrow\downarrow}(k) + X_{ee}^{\uparrow\downarrow}(k)\big] - \frac{\rho^\uparrow}{\rho}\delta_1 X_{ed}^{\uparrow\downarrow}(k), \tag{A19}$$

$$\mathcal{L}_3 = \beta_2\left[1 - \frac{\rho^\uparrow}{\rho}X_{ed}^{\uparrow\uparrow}(k)\right] - \frac{\rho^\downarrow\rho^{\uparrow 2}}{\rho^3}\big[X_{dd}^{\uparrow\downarrow}(k)X_{dd}^{\downarrow\uparrow}(k) - X_{dd}^{\uparrow\uparrow}(k)X_{dd}^{\downarrow\downarrow}(k)\big] \times\big[X_{ed}^{\uparrow\uparrow}(k) + X_{ee}^{\uparrow\uparrow}(k)\big] + \frac{\rho^\downarrow}{\rho}\beta_1 X_{ed}^{\uparrow\downarrow}(k), \tag{A20}$$

$$\mathcal{L}_4 = -\frac{\rho^\uparrow}{\rho}\delta_2\big[X_{ed}^{\uparrow\uparrow}(k) + X_{ee}^{\uparrow\uparrow}(k)\big] - \frac{\rho^\downarrow}{\rho}\beta_2\big[X_{ed}^{\uparrow\downarrow}(k) + X_{ee}^{\uparrow\downarrow}(k)\big] + \frac{\rho^\downarrow}{\rho}P(k)X_{ed}^{\uparrow\downarrow}(k). \tag{A21}$$

Notations R_j and C_j ($j = 1,2,3$), respectively, are given by

$$R_1 = \left\{\frac{\rho^\uparrow}{\rho}b_1\big[X_{ed}^{\uparrow\uparrow}(k) + X_{ee}^{\uparrow\uparrow}(k)\big] - \frac{\rho^\downarrow}{\rho}b_2\big[X_{ed}^{\uparrow\downarrow}(k) + X_{ee}^{\uparrow\downarrow}(k)\big]\right\}\left[1 - \frac{\rho^\downarrow}{\rho}X_{ed}^{\downarrow\downarrow}(k)\right] + \frac{\rho^\uparrow\rho^\downarrow}{\rho^2}\left\{b_1 X_{ed}^{\uparrow\downarrow}(k) + \frac{\rho^\downarrow}{\rho}X_{dd}^{\downarrow\downarrow}(k)\big[X_{ed}^{\uparrow\downarrow}(k) + X_{ee}^{\uparrow\downarrow}(k)\big]\right\}\big[X_{ed}^{\downarrow\uparrow}(k) + X_{ee}^{\uparrow\downarrow}(k)\big] - \frac{\rho^\uparrow\rho^\downarrow}{\rho^2}\left\{b_2 X_{ed}^{\uparrow\downarrow}(k) + \frac{\rho^\downarrow}{\rho}X_{dd}^{\downarrow\downarrow}(k)\big[X_{ed}^{\uparrow\uparrow}(k) + X_{ee}^{\uparrow\uparrow}(k)\big]\right\}\big[X_{ed}^{\downarrow\downarrow}(k) + X_{ee}^{\downarrow\downarrow}(k)\big], \tag{A22}$$

$$R_2 = \left\{\frac{\rho^\downarrow}{\rho}a_2\big[X_{ed}^{\uparrow\downarrow}(k) + X_{ee}^{\uparrow\downarrow}(k)\big] - \frac{\rho^\uparrow}{\rho}a_1\big[X_{ed}^{\uparrow\uparrow}(k) + X_{ee}^{\uparrow\uparrow}(k)\big]\right\}\left[1 - \frac{\rho^\downarrow}{\rho}X_{ed}^{\downarrow\downarrow}(k)\right] - \frac{\rho^\uparrow\rho^\downarrow}{\rho^2}\left\{a_1 X_{ed}^{\uparrow\downarrow}(k) + \frac{\rho^\downarrow}{\rho}X_{dd}^{\uparrow\downarrow}(k)\big[X_{ed}^{\uparrow\downarrow}(k) + X_{ee}^{\uparrow\downarrow}(k)\big]\right\}\big[X_{ed}^{\downarrow\uparrow}(k) + X_{ee}^{\uparrow\downarrow}(k)\big] + \frac{\rho^{\downarrow 2}}{\rho^2}\left\{a_2 X_{ed}^{\uparrow\downarrow}(k) + \frac{\rho^\uparrow}{\rho}X_{dd}^{\uparrow\downarrow}(k)\big[X_{ed}^{\uparrow\uparrow}(k) + X_{ee}^{\uparrow\uparrow}(k)\big]\right\}\big[X_{ed}^{\downarrow\downarrow}(k) + X_{ee}^{\downarrow\downarrow}(k)\big], \tag{A23}$$

$$R_3 = -P(k)\left[1 - \frac{\rho^\downarrow}{\rho}X_{ed}^{\downarrow\downarrow}(k)\right] - \frac{\rho^\uparrow}{\rho}\delta_2\big[X_{ed}^{\uparrow\downarrow}(k) + X_{ee}^{\uparrow\downarrow}(k)\big] - \frac{\rho^\downarrow}{\rho}\beta_2\big[X_{ed}^{\downarrow\downarrow}(k) + X_{ee}^{\downarrow\downarrow}(k)\big], \tag{A24}$$

$$C_1 = \frac{\rho^\uparrow}{\rho}\left\{b_1\left[1 - \frac{\rho^\uparrow}{\rho}X_{ed}^{\uparrow\uparrow}(k)\right] - \frac{\rho^\uparrow\rho^\downarrow}{\rho^2}X_{dd}^{\downarrow\uparrow}(k)\big[X_{ed}^{\uparrow\downarrow}(k) + X_{ee}^{\uparrow\downarrow}(k)\big]\right\}\big[X_{ed}^{\downarrow\uparrow}(k) + X_{ee}^{\uparrow\downarrow}(k)\big] + \frac{\rho^\downarrow}{\rho}\left\{\frac{\rho^\uparrow}{\rho}X_{dd}^{\downarrow\uparrow}(k)\big[X_{ed}^{\uparrow\uparrow}(k) + X_{ee}^{\uparrow\uparrow}(k)\big] - b_2\left[1 - \frac{\rho^\uparrow}{\rho}X_{ed}^{\uparrow\uparrow}(k)\right]\right\}\big[X_{ed}^{\downarrow\downarrow}(k) + X_{ee}^{\downarrow\downarrow}(k)\big] + \frac{\rho^\uparrow}{\rho}\left\{\frac{\rho^\uparrow}{\rho}b_1\big[X_{ed}^{\uparrow\uparrow}(k) + X_{ee}^{\uparrow\uparrow}(k)\big] - \frac{\rho^\downarrow}{\rho}b_2\big[X_{ed}^{\uparrow\downarrow}(k) + X_{ee}^{\uparrow\downarrow}(k)\big]\right\}X_{dd}^{\downarrow\uparrow}(k), \tag{A25}$$

$$C_2 = \frac{\rho^\uparrow}{\rho}\left\{\frac{\rho^\uparrow\rho^\downarrow}{\rho^2}X_{dd}^{\uparrow\uparrow}(k)\big[X_{ed}^{\uparrow\downarrow}(k) + X_{ee}^{\uparrow\downarrow}(k)\big] - a_1\left[1 - \frac{\rho^\uparrow}{\rho}X_{ed}^{\uparrow\uparrow}(k)\right]\right\}\big[X_{ed}^{\downarrow\uparrow}(k) + X_{ee}^{\uparrow\downarrow}(k)\big] + \frac{\rho^\downarrow}{\rho}\left\{a_2\left[1 - \frac{\rho^\uparrow}{\rho}X_{ed}^{\uparrow\uparrow}(k)\right] - \frac{\rho^{\uparrow 2}}{\rho^2}X_{dd}^{\uparrow\uparrow}(k)\big[X_{ed}^{\uparrow\uparrow}(k) + X_{ee}^{\uparrow\uparrow}(k)\big]\right\}\big[X_{ed}^{\downarrow\downarrow}(k) + X_{ee}^{\downarrow\downarrow}(k)\big] + \frac{\rho^\uparrow}{\rho}\left\{\frac{\rho^\downarrow}{\rho}a_1\big[X_{ed}^{\uparrow\downarrow}(k) + X_{ee}^{\uparrow\downarrow}(k)\big] - \frac{\rho^\uparrow}{\rho}a_1\big[X_{ed}^{\uparrow\uparrow}(k) + X_{ee}^{\uparrow\uparrow}(k)\big]\right\}X_{ed}^{\downarrow\uparrow}(k), \tag{A26}$$

$$C_3 = \frac{\rho^{\uparrow}}{\rho}\delta_1\left[X_{ed}^{\downarrow\downarrow}(k) + X_{ee}^{\downarrow\downarrow}(k)\right] + \frac{\rho^{\downarrow}}{\rho}\beta_1\left[X_{ed}^{\downarrow\downarrow}(k) + X_{ee}^{\downarrow\downarrow}(k)\right] - \frac{\rho^{\uparrow}}{\rho}P(k)X_{ed}^{\downarrow\uparrow}(k). \quad \text{(A27)}$$

[1] D. C. Tsui, H. L. Störmer, and A. C. Gossard, Phys. Rev. Lett. **48**, 1559 (1982).
[2] *The Fractional Quantum Hall Effect*, edited by T. Chakraborty and P. Pietiläinen (Springer-Verlag, New York, 1988); *The Quantum Hall Effect*, edited by R. E. Prange and S. M. Girvin (Springer-Verlag, New York, 1990).
[3] R. B. Laughlin, Phys. Rev. Lett. **50**, 1395 (1983).
[4] B. I. Halperin, Helv. Phys. Acta **56**, 75 (1983).
[5] T. Chakraborty and F. C. Zhang, Phys. Rev. B **29**, 7032 (1984).
[6] F. C. Zhang and T. Chakraborty, Phys. Rev. B **30**, 7320 (1984).
[7] T. Chakraborty and P. Pietiläinen, Phys. Rev. B **41**, 10862 (1990).
[8] E. H. Rezayi, Phys. Rev. B **36**, 5454 (1987).
[9] X. C. Xie, Y. Guo, and F. C. Zhang, Phys. Rev. B **40**, 3487 (1989).
[10] X. C. Xie and F. C. Zhang, Mod. Phys. Lett. B **5**, 471 (1991).
[11] P. A. Maksym, J. Phys. Condens. Matter **1**, 6299 (1989).
[12] X. G. Wu, G. Dev, and J. K. Jain, Phys. Rev. Lett. **71**, 153 (1993).
[13] R. G. Clark, S. R. Haynes, A. M. Suckling, J. R. Mallett, P. A. Wright, J. J. Harris, and C. T. Foxon, Phys. Rev. Lett. **62**, 1536 (1989).
[14] J. P. Eisenstein, H. L. Stormer, L. N. Pfeiffer, and K. W. West, Phys. Rev. Lett. **62**, 1540 (1989).
[15] J. P. Eisenstein, H. L. Stormer, L. N. Pfeiffer, and K. W. West, Phys. Rev. B **41**, 7910 (1990).
[16] L. W. Engel, S. W. Hwang, T. Sajoto, D. C. Tsui, and M. Shayegan, Phys. Rev. B **45**, 3418 (1992).
[17] R. R. Du, A. S. Yeh, H. L. Stormer, D. C. Tsui, L. N. Pfeiffer, and K. W. West, Phys. Rev. Lett. **75**, 3926 (1995).
[18] R. R. Du, A. S. Yeh, H. L. Stormer, D. C. Tsui, L. N. Pfeiffer, and K. W. West, Phys. Rev. B **55**, R7351 (1997).
[19] R. J. Nicholas, D. R. Leadley, M. S. Daly, M. van der Burgt, P. Gee, J. Singleton, D. K. Maude, J. C. Portal, J. J. Harris, and C. T. Foxon, Semicond. Sci. Technol. **11**, 1477 (1996).
[20] I. V. Kukushkin, K. von Klitzing, and K. Eberl, Phys. Rev. Lett. **82**, 3665 (1999).
[21] S. Melinte, N. Freytag, M. Horvatić, C. Berthier, L. P. Lévy, V. Bayot, and M. Shayeǵan, Phys. Rev. Lett. **84**, 354 (2000).
[22] A. E. Dementyev, N. N. Kuzma, P. Khandelwal, S. E. Barrett, L. N. Pfeiffer, and K. W. West, Phys. Rev. Lett. **83**, 5074 (1999).
[23] H. L. Störmer, A. S. Yeh, W. Pan, D. C. Tsui, L. N. Pfeiffer, K. W. Baldwin, and K. W. West, Physica E (Amsterdam) **3**, 38 (1998).
[24] W. Pan, H. L. Störmer, D. C. Tsui, L. N. Pfeiffer, K. W. Baldwin, and K. W. West, Phys. Rev. Lett. **90**, 016801 (2003).
[25] W. Pan, K. W. Baldwin, K. W. West, L. N. Pfeiffer, and D. C. Tsui, Phys. Rev. B **91**, 041301(R) (2015).
[26] V. Bellani, F. Dionigi, F. Rossella, M. Amado, E. Diez, G. Biasiol, and L. Sorba, Phys. Rev. B **81**, 155316 (2010).
[27] N. Samkharadze, I. Arnold, L. N. Pfeiffer, K. W. West, and G. A. Csathy, Phys. Rev. B **91**, 081109(R) (2015).
[28] Irene Dujovne *et al.*, Phys. Rev. Lett. **90**, 036803 (2003).
[29] L. A. Tracy, J. P. Eisenstein, L. N. Pfeiffer, and K. W. West, Phys. Rev. Lett. **98**, 086801 (2007).
[30] V. V. Vanovsky, V. S. Khrapai, A. A. Shashkin, V. Pellegrini, L. Sorba, and G. Biasiol, Phys. Rev. B **87**, 081306(R) (2013).
[31] J. H. Smet, R. Deutschmann, W. Wegscheider, G. Abstreiter, and K. von Klitzing, Phys. Rev. Lett. **86**, 2412 (2001).
[32] J. K. Jain, Phys. Rev. Lett. **63**, 199 (1989).
[33] A. Lopez and E. Fradkin, Phys. Rev. B **44**, 5246 (1991).
[34] V. Kalmeyer and S. C. Zhang, Phys. Rev. B **46**, 9889 (1992).
[35] B. I. Halperin, P. A. Lee, and N. Read, Phys. Rev. B **47**, 7312 (1993).
[36] S. S. Mandal and J. K. Jain, Phys. Rev. B **66**, 155302 (2002); S. Y. Lee, V. W. Scarola, and J. K. Jain, *ibid.* **66**, 085336 (2002); C. C. Chang, S. S. Mandal, and J. K. Jain, *ibid.* **67**, 121305(R) (2003); C. C. Chang and J. K. Jain, Phys. Rev. Lett. **92**, 196806 (2004).
[37] R. K. Kamilla and J. K. Jain, Phys. Rev. B **55**, 9824 (1997).
[38] S. Fantoni, Nuovo Climento A **44**, 191 (1978).
[39] M. L. Ristig, From nuclei to particles in *Proceedings of the International School of Physics "Enrico Fermi," Course LVII, Varenna 1981*, edited by A. Molinari (North Holland, Amsterdam, 1982); M. L. Ristig, Z. Phys. B **79**, 351 (1990).
[40] K. Park and J. K. Jain, Phys. Rev. B **62**, R13274 (2000).
[41] S. Mukherjee, S. S. Mandal, Ying-Hai Wu, A. Wojs, and J. K. Jain, Phys. Rev. Lett. **112**, 016801 (2014).
[42] J. K. Jain and R. K. Kamilla, Phys. Rev. B **55**, R4895 (1997).
[43] R. Morf and B. I. Halperin, Phys. Rev. B **33**, 2221 (1986); R. Morf, N. d'Ambrumenil, and B. I. Halperin, *ibid.* **34**, 3037 (1986).
[44] M. W. C. Dharma-Wardana, Phys. Rev. B **51**, 1653 (1995).
[45] S. Mukherjee, S. S. Mandal, A. Wójs, and J. K. Jain, Phys. Rev. Lett. **109**, 256801 (2012); S. Mukherjee, J. K. Jain, and S. S. Mandal, Phys. Rev. B **90**, 121305(R) (2014).
[46] S. Mukherjee and S. S. Mandal, Phys. Rev. B **92**, 235302 (2015).
[47] Ajit C. Balram, Phys. Rev. B **94**, 165303 (2016).
[48] O. Ciftja and S. Fantoni, Phys. Rev. B **58**, 7898 (1998); O. Ciftja, *ibid.* **59**, 10194 (1999).
[49] G. Fano, F. Ortolani, and E. Tosatti, Nuovo Cimento D **9**, 1337 (1987).
[50] S. Modak, S. S. Mandal, and K. Sengupta, Phys. Rev. B **84**, 165118 (2011).